Self-association of CPV3, an avian thymic parvalbumin

Michael T. Henzl[a,*], Hongmei Zhao[a], Cristian T. Saez[b]

[a]*Biochemistry Department, 117 Schweitzer Hall, University of Missouri at Columbia, Columbia, MO 65211, USA*
[b]*Division of Biochemistry and Molecular Biology, University of Missouri at Kansas City, Kansas City, MO, USA*

Received 21 July 1995; revised version received 4 October 1995

Abstract The avian parvalbumin called CPV3 readily forms disulfide-linked oligomers. Sedimentation data presented herein reveal that CPV3 also undergoes noncovalent self-association. Interestingly, the noncovalent interaction is promoted by either Ca^{2+} or Mg^{2+}, whereas covalent complex formation displays an absolute requirement for the Ca^{2+}-bound protein. Apo-CPV3 exhibits an apparent sedimentation coefficient of 2.08 S at 20°C, in 0.15 M NaCl, 0.025 M HEPES-NaOH, pH 7.4. This value increases to 2.85 S or 3.16 S with addition of 1.0 mM Ca^{2+} or 5.0 mM Mg^{2+}, respectively. Least-squares analysis of sedimentation equilibrium data suggests that 100 μM apo-CPV3 is primarily a mixture of monomeric and dimeric forms. With the addition of Ca^{2+}, the equilibrium becomes exclusively monomer–trimer, with negligible amounts of dimer. A comparable distribution is observed in the presence of Mg^{2+}.

Key words: Analytical ultracentrifugation; Association; Ca^{2+}-binding protein; Parvalbumin; Sedimentation

1. Introduction

Parvalbumins are small (M_r = 12,000), vertebrate-specific relatives of calmodulin. They are commonly regarded as cytosolic Ca^{2+} buffers that function in myofibrillar relaxation and neuronal de-excitation (for reviews, see [1–3]). There is circumstantial evidence, however, that select isoforms may play alternative biological roles. For example, the mammalian oncofetal parvalbumin known as oncomodulin [4,5] may act as a Ca^{2+}-dependent regulatory protein during early embryonic development and tumorigenesis [6].

Whereas lower vertebrates — fish and amphibians — express multiple parvalbumins in skeletal muscle, birds and postnatal mammals express a single muscle isoform. Interestingly, avian species have retained two additional parvalbumin isoforms that are expressed exclusively in thymus tissue. Avian thymic hormone (ATH) was discovered and characterized by Ragland and colleagues [7,8]. The name of the protein, bestowed several years before it was recognized as a parvalbumin, reflects its capacity to influence T-cell maturation and proliferation [9,10]. ATH is produced, and presumably secreted, by select cortical epithelial cells [11,12]. The other thymus-specific isoform, CPV3, was discovered six years ago in our laboratory [13]. Recent immunofluorescence studies have revealed that CPV3 and ATH are expressed by a common epithelial population (R.C. Hapak and M.T. Henzl, unpublished observations). Although the biological significance of these two proteins is presently unknown, their thymus-specific expression implies participation in some aspect of avian immune function.

In addition to its atypical tissue distribution, CPV3 displays several other distinctive features. Whereas parvalbumin metal ion-binding sites generally appear equivalent in titrations with Ca^{2+} or Mg^{2+} (e.g. [14–16]), the two sites in CPV3 exhibit distinctly different affinities for the ions [17]. In this regard, CPV3 resembles oncomodulin, with which it shares a high degree of sequence identity (74 of 108 residues) [17]. Moreover, CPV3 contains two cysteine residues, one of which — cysteine-72 —is predicted to be solvent-accessible in the Ca^{2+}-bound form. Accordingly, we find that the Ca^{2+}-bound form of CPV3 readily forms disulfide-linked oligomers in the absence of thiol-protecting reagents [18]. Importantly, neither the apo- nor Mg^{2+}-bound forms of the protein exhibit this tendency.

We have recently learned that CPV3 displays unusual behavior in certain calorimetric experiments (H. Zhao and M.T. Henzl, unpublished observations). When the binding of Ca^{2+} is monitored by titration calorimetry, anomalous exotherms are observed late in the titration. Furthermore, the denaturation of Ca^{2+}- or Mg^{2+}-bound CPV3, as monitored by differential scanning calorimetry, clearly involves multiple transitions. Reasoning that these phenomena might reflect metal ion-promoted noncovalent association, we have examined the sedimentation properties of CPV3 in the apo-, Ca^{2+}-bound, and Mg^{2+}-bound forms.

2. Materials and methods

Recombinant CPV3 was isolated in the presence of dithiothreitol (DTT) by methods described previously [17]. The purified protein appeared homogeneous when visualized with Coomassie blue R250 following SDS-PAGE. Removal of the reductant was necessary prior to the sedimentation studies, since oxidized DTT absorbs strongly between 260 and 280 nm. Moreover, since we wished to examine the influence of metal ions on sedimentation behavior, it was desirable to employ the apo-form of the protein. DTT was removed by gel-filtration on Sephadex G-25, and bound Ca^{2+} was removed by passage over EDTA-agarose [19] as described previously [20]. Both columns were equilibrated with deoxygenated buffer prior to loading. The eluate from the G-25 column was passed through an EDTA-agarose column connected in tandem. Elution of the protein from the latter was monitored with a UV-absorbance detector. The DTT-free, apo-protein was collected in an N_2-filled serum bottle and subsequently concentrated in an Amicon ultrafiltration cell (purged with N_2 prior to introducing the sample) to approximately 0.5 mM. This solution was divided into 2.0 ml aliquots which were placed in N_2-filled serum bottles, quick-frozen in dry-ice/EtOH, and stored at −80°C.

Samples of the protein were tested for sulfhydryl content and residual Ca^{2+}. The sulfhydryl content, measured with a minor modification of the Ellman's test [21], was determined to be 2.0 mol –SH/mol protein. The residual Ca^{2+}, measured by flame atomic absorption spectrometry, was determined to be less than 0.02 mol Ca^{2+}/mol of protein.

Analytical ultracentrifugation was performed at 20°C in a Beckman Model XL-A analytical ultracentrifuge. The radial protein distribution was determined by UV absorbance at either 258 or 280 nm. The XL-A

*Corresponding author. Fax: (1) (314) 884-4812.
E-mail: bchenzl@muccmail.missouri.edu

SSDI 0014-5793(95)01202-8

acquires the absorbance data at 0.001 cm intervals and stores them as ASCII files. The buffer employed in both velocity and equilibrium analyses consisted of 0.15 M NaCl, 0.025 M HEPES-NaOH, pH 7.4.

Sedimentation velocity samples were examined in standard double-sector cells. The Beckman An-60 four-hole titanium rotor accomodates three cells plus a counter-weight, permitting simultaneous analysis of apo-, Ca^{2+}-, and Mg^{2+}-bound samples. Samples employed for sedimentation equilibrium samples were loaded into six-channel Yphantis cells. The six-channel design accomodates three different concentrations of CPV3 and corresponding buffer blanks. The use of the six-channel cells, in combination with the An-60 rotor, enabled us to examine CPV3 at three concentrations in the apo-, Ca^{2+}-, and Mg^{2+}-bound forms.

Nonlinear least-squares analysis. The procedure used to model the CPV3 association reaction is based on the method employed by Lewis and Youle to model ricin subunit association [22]. Radial absorbance data were imported into the SCIENTIST® program from Micro-Math, Inc (Salt Lake City, UT). In contrast to many least-squares minimization programs, the mathematical models employed for fitting need not be reduced to a single analytical expression. Rather, they may consist of systems of equations harboring one or more implicit variables. The minimization procedure employed by SCIENTIST is based on a modification of Powell's algorithm. Statistical analysis of the fitted parameters and the quality of fit were evaluated with the statistics package supplied with the program. Optimized parameter values are reported plus-or-minus the standard deviation. Analyses were performed on a desktop computer equipped with an 80486 processor and math co-processor.

3. Results

3.1. Sedimentation velocity

100 μM samples of CPV3 were subjected to boundary sedimentation velocity analysis at 20°C with a rotor speed of 40,000 rpm, under solution conditions designed to yield the apo-, Ca^{2+}-bound, or Mg^{2+}-bound forms of the protein. The absorbance in the cell was measured as a function of radial distance at 30-min intervals. The resulting family of absorbance traces is shown in Fig. 1 for the apo- (panel A), Ca^{2+}-bound (panel B), and Mg^{2+}-bound (panel C) forms of CPV3. Note that the protein exhibits a pronounced increase in sedimentation rate in the presence of Ca^{2+} or Mg^{2+}. The sedimentation boundaries display no overt evidence of heterogeneity — indicating either that there is a single sedimenting species or, if there are multiple species, that they are in facile equilibrium.

The change in the position of the boundary position, r_b, with time is given by the following equation

$$\frac{dr_b}{dt} = s\omega^2 r_b \quad (1)$$

where s is the sedimentation coefficient, t is the time in seconds, and ω is the angular velocity in rad/s (e.g. [23]). Integration yields

$$\ln r_b = s\omega^2 t + C \quad (2)$$

where C is simply a constant of integration. In Fig. 2A, the logarithm of the boundary position has been plotted vs. $\omega^2 t$, for each of the three forms of CPV3. The solid lines represent the best least-squares fit to Eqn. 2. In each case, the slope of the line is equal to s. The apo-protein (○) displays an apparent sedimentation coefficient of 2.08 S, somewhat larger than would be anticipated for monomeric CPV3, a roughly spherical molecule with M_r = 11,977. For comparison, lysozyme (M_r = 14.300) and myoglobin (M_r = 17.800) exhibit sedimentation coefficients of 1.91 S and 1.97 S, respectively [24].

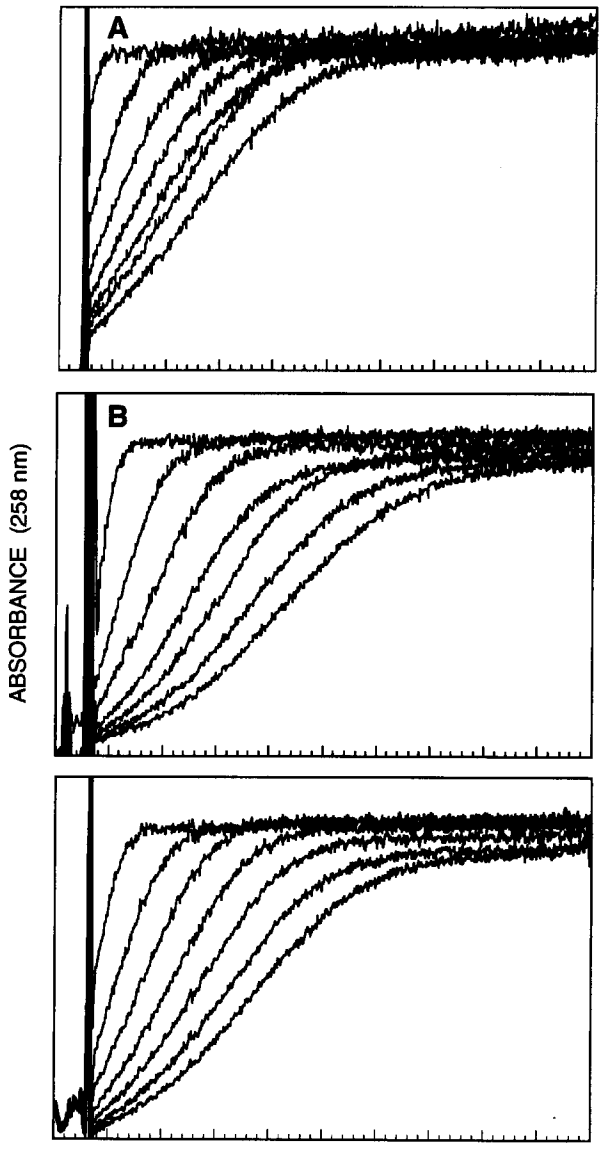

Fig. 1. Influence of Ca^{2+} and Mg^{2+} on CPV3 sedimentation rate. The samples employed for this analysis consisted of 100 μM CPV3 in 0.15 M NaCl, 0.025 M HEPES-NaOH, pH 7.4, with the following additions: (A) 5.0 mM EDTA; (B) 1.0 mM Ca^{2+}; (C) 5.0 mM Mg^{2+}.

In the presence of 1.0 mM Ca^{2+} (△), the sedimentation coefficient increases to 2.85 S, a value more typical of a substantially larger protein. Elastase (M_r = 24,600) and subtilisin (M_r = 27,500), for example, display sedimentation coefficients of 2.6 and 2.77, respectively [24]. Similarly, in the presence of 5 mM Mg^{2+} (□), the apparent sedimentation coefficient increases to 3.16 S. For comparison, carbonic anhydrase (28,800) and superoxide dismutase (M_r = 33,900) exhibit sedimentation coefficients of 3.23 and 3.35, respectively [24]. Thus, the sedimentation coefficients observed for CPV3 in the presence of Ca^{2+} or Mg^{2+} are more characteristic of globular proteins having molecular weights 2–3 times that of the monomer. This finding suggests that the metal ions promote self-association of CPV3.

Sedimentation equilibrium studies were performed to gain

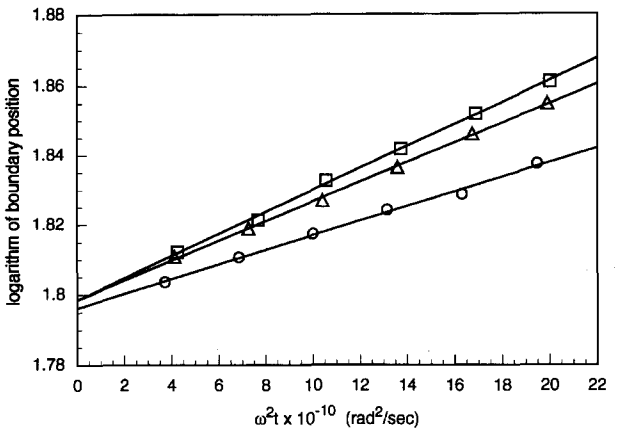

Fig. 2. Analysis of sedimentation velocity data. Boundary mid-points for the data presented in Fig. 1 have been plotted vs. $\omega^2 t$ for apo- (○), Ca^{2+}- bound (△), and Mg^{2+}-bound CPV3 (□). The solid lines through the data represent the best least-squares fit to the data. The R^2-values for the three lines are 0.996, 0.999, and 0.998, respectively.

further insight into the phenomenon. Samples of CPV3 were prepared for ultracentrifugation at concentrations of 100 μM, 200 μM, and 400 μM — in the presence of EDTA, Ca^{2+}, or Mg^{2+}. Centrifugation was carried out at 25,000 rpm for 72 h. The radial scans acquired at 48 and 72 h were superimposible, indicating that equilibrium had been attained.

Absorbance is plotted as a function of the radial displacement in Fig. 3 for the 200 μM samples. Notice that the meniscus concentration is higher in the cell containing the apo-sample (panel A) and that the curvature in the absorbance scan is less pronounced than for the Ca^{2+} (panel C) and Mg^{2+} samples (panel E). Both observations are consistent with a higher average molecular weight in the presence of metal ion.

For a monodisperse system, the solute concentration (c) is related to the radial displacement (r) according to Eqn. 3:

$$c = c_a * \exp\left[\left(\frac{M*(1-\rho\bar{v})\omega^2}{2RT}\right)*(r^2 - r_a^2)\right] \quad (3)$$

where r_a and c_a are the radial displacement and concentration at the meniscus, M is the average molecular weight, ρ is the solution density, $\bar{v}$ is the partial specific volume of the protein, ω is the angular velocity, R is the gas constant (8.314×10^7 erg·mol^{-1}·K^{-1}), and T is the absolute temperature (e.g. [23]). The solution density was determined to be 1.02 g/ml, and the partial specific volume of CPV3 was assumed to be 0.73 cm^3/g. The three datasets displayed in Fig. 3 were treated with this model, treating M as a variable parameter. This procedure yielded estimates for M of 20.4×10^3, 26.7×10^3, and 28.4×10^3 for the apo-, Ca^{2+}-bound, Mg^{2+}-bound samples, respectively. These values, all substantially higher than the monomer molecular weight, are entirely consistent with the sedimentation velocity data and are indicative of self-association.

Notice, however, that the agreement between the observed and calculated data obtained with this simple model is unsatisfactory, as evidenced by the systematic variation in the residuals (Fig. 3B,D,F,E). The poor correlation arises because Eqn. 3 describes the distribution of a single species, whereas self-association in fact generates several species that differ substantially in molecular weight and, therefore, distribute nonuniformly under the influence of the gravitational field.

Further insight into the interaction between CPV3 monomers can be obtained by applying a model that explicitly includes association of the CPV3 to form dimers and trimers. The association reaction is assumed to proceed via a stepwise mechanism:

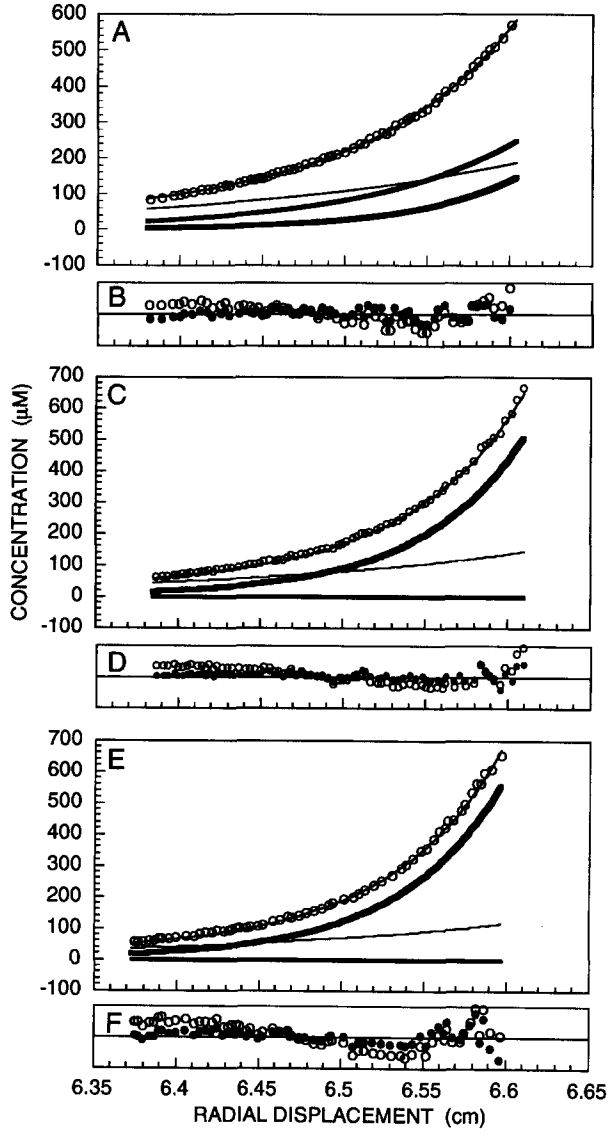

Fig. 3. Influence of Ca^{2+} and Mg^{2+} on CPV3 sedimentation equilibrium behavior. Samples of CPV3 were subjected to sedimentation equilibrium analysis as described in the text. Data are presented for 200 μM CPV3 in the absence and presence of Ca^{2+} or Mg^{2+}. (A) 5.0 mM EDTA. The solid line through the data points corresponds to the best fit obtained with the self-association model described by Eqn. 7. The fine, medium, and thick lines below the data depict the calculated distributions of the monomeric, dimeric, and trimeric species, respectively. Residuals for the fit are shown in (B) (●), along with the residuals obtained for the fit to Eqn. 3 (○). (C) 2.0 mM Ca^{2+}. The format is identical to that in (A). Residuals for the least-squares fits to Eqn. 3 (○) and Eqn. 7 (●) are displayed in (D). (E) 10 mM Mg^{2+}. Format is identical to that described in (A). Residuals for fits to Eqn. 3 (○) and Eqn. 7 (●) are presented in (F).

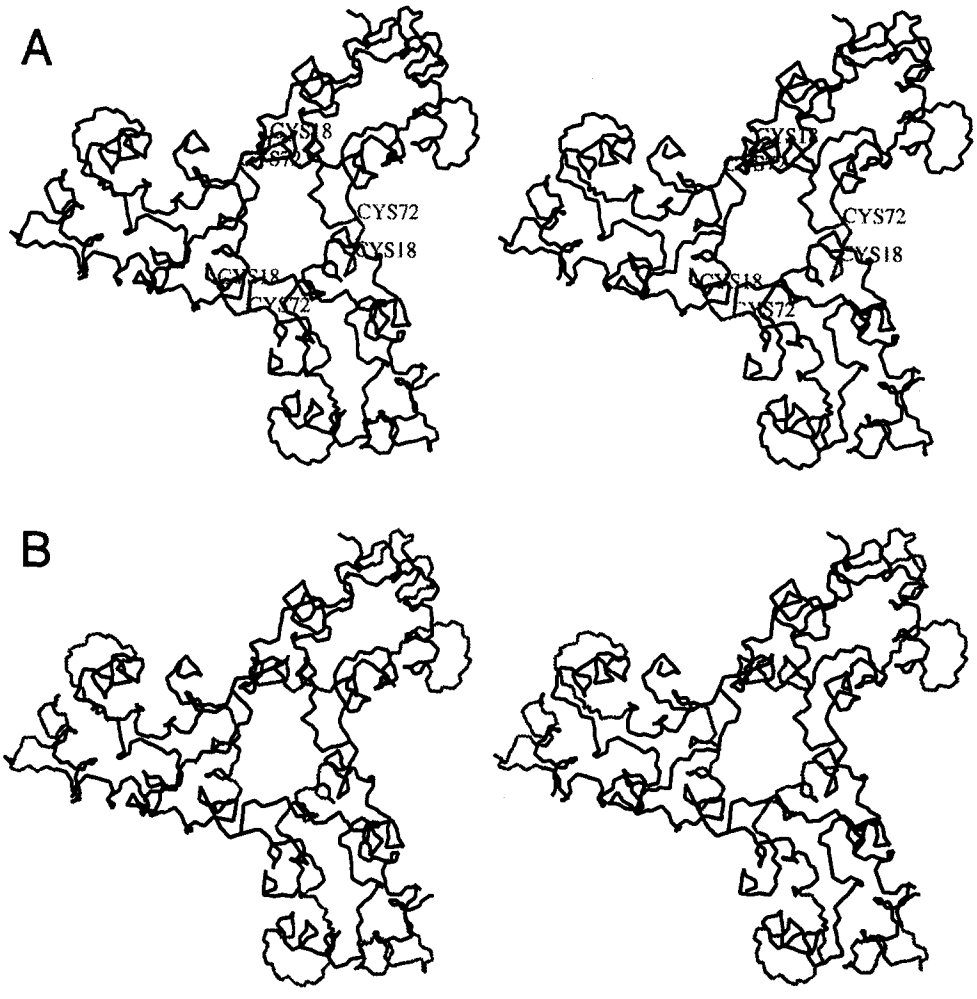

Fig. 4. Hypothetical model of the CPV3 trimer. The oncomodulin peptide backbone was employed as a CPV3 surrogate for this exercise. Three copies 'CPV3' were aligned so as to bring C18 and C72 from adjacent monomers into sufficient proximity to allow disulfide bond formation. The monomer positions were then adjusted to eliminate most of the unfavorable contacts. Two views of the putative complex are presented, looking down the three-fold symmetry axis. (A) C18 and C72 are depicted in gray, and the disulfide bonds have been retained. (B) The disulfide bonds have been omitted, and the A helices and Ca^{2+}-binding loops have been shown in gray for purposes of orientation.

$$P + P \xrightarrow{K_2} P_2 + P \xrightarrow{K_3} P_3 \tag{4}$$

where P represents the CPV3 monomer. The equilibrium constants for formation of the dimeric and trimeric species — K_2 and K_3, respectively — are then given by the following expressions:

$$K_2 = \frac{[P_2]}{[P]^2} \text{ and } K_3 = \frac{[P_3]}{[P_2][P]} \tag{5}$$

from which it follows that

$$[P_2] = K_2[P]^2 \text{ and } [P_3] = K_3K_2[P]^3 \tag{6}$$

The total concentration of CPV3 at any point in the sedimentation cell must of course equal the contributions from the monomer, dimer, and trimer. Each species will exhibit a radial distribution of the form give by Eqn. 3. If we substitute c_a, the concentration of monomer at the meniscus, for $[P]$ in the expressions for $[P_2]$ and $[P_3]$ given in Eqn. 6, we obtain the following expression for the total solute concentration as a function of radial displacement:

$$\begin{aligned} c = c_a * \exp\left[\left(\frac{M(1-\rho\bar{v})\omega^2}{2RT}\right) * (r^2 - r_a^2)\right] + \\ + 2\beta_2 c_a^2 * \exp\left[\left(\frac{2M(1-\rho\bar{v})\omega^2}{2RT}\right) * (r^2 - r_a^2)\right] + \\ + 3\beta_3 c_a^3 * \exp\left[\left(\frac{3M(1-\rho\bar{v})\omega^2}{2RT}\right) * (r^2 - r_a^2)\right] \end{aligned} \tag{7}$$

The first, second, and third terms in Eqn. 7 describe the radial distributions of the monomeric, dimeric, and trimeric species, respectively. Notice that we have replaced the stepwise equilibrium constants by overall association constants, β_2 and β_3, where $\beta_3 = K_2 \times K_3$. Notice further that the latter two terms

have been multiplied by factors of 2 and 3 to account for the presence of two or three protein monomers in the dimeric and trimeric complexes, respectively. M is the CPV3 monomer weight (11,977). β_2, β_3, and c_a are the variable parameters in this model. Other than requiring that they be nonnegative, they were unconstrained. Prior to performing least-squares minimization with this model, the absorbance data in the sedimentation equilibrium files were converted to molarity, employing the extinction coefficient for the monomer at 280 nm. Deviations in the extinction coefficient resulting from association were assumed to be negligible.

Application of this model to the data obtained with the 200 μM sample of apo-CPV3 yielded $\beta_2 = 3.5(\pm 0.5) \times 10^3$ M^{-1} and $\beta_3 = 7.4(\pm 0.2) \times 10^6$ M^{-2}. The solid line through the data in Fig. 3A depicts the calculated protein distribution obtained with these values. The residuals for this fit are shown in Fig. 3B (●). Notice that the distribution of the residuals is more random than that obtained with Eqn. 3 (○), indicative of an improved fit to the data. The R^2 value for this fit is 0.9999. The radial distributions of the monomeric, dimeric, and trimeric species are indicated in Fig. 3A by the fine, medium, and thick solid lines, respectively.

When the model given by Eqn. 7 is applied to the corresponding data for the Ca^{2+}-bound sample, $\beta_2 = 0$ and $\beta_3 = 5.7(\pm 0.8) \times 10^7$ M^{-2}. Calculated data, obtained with these values, are represented by the solid line through the data points in Fig. 3C. The distribution of the residuals for this fit are shown in panel D (●). R^2 for this fit was 0.9997. This result contrasts markedly with the corresponding apo-protein analysis. Whereas the dimeric form was the predominant species in the apo-preparation, its concentration is negligible in the presence of Ca^{2+}. The implication is that dimeric species are rapidly converted to trimers when CPV3 is in the Ca^{2+}-bound state, so that their steady-state dimer concentration is essentially zero.

Qualitatively similar results are obtained when the model specified by Eqn. 7 is applied to the data for Mg^{2+}-bound CPV3. Once again, the least-squares minimization indicates that $\beta_2 = 0$. However, the value returned for β_3 is somewhat larger, approximately 1.2×10^8 M^{-2}. The R^2 value for this fit was 0.9985.

4. Discussion

These data indicate that CPV3 undergoes self-association and that the nature of the association is strongly influenced by the divalent cations, Ca^{2+} and Mg^{2+}. This result is rather unexpected, since parvalbumins are generally regarded as highly soluble, monomeric species. For example, pike parvalbumin has been examined by NMR at concentrations as high as 15 mM [25], and we have performed NMR studies on 8 mM solutions of oncomodulin [26]. No indication of aggregation was observed in either case.

The sedimentation coefficient determined for the apo-protein (2.08 S) is uncharacteristically large for a protein with M_r = 12,000. Correspondingly, the apo-protein exhibits an apparent average molecular weight of 20,400 by sedimentation equilibrium data. Nonlinear least-squares analysis implies that CPV3 exists predominantly in the monomeric and dimeric forms in the absence of divalent cations. The overall association constants for dimerization and trimerization of apo-CPV3 are 3.5×10^3 M^{-1} and 7.4×10^6 M^{-2}, respectively. At a total CPV3 concentration of 100 μM, the levels of monomer, dimer, and trimer are predicted to be 65 μM, 30 μM, and 5 μM, respectively. These species are in facile equilibrium, as judged by the homogeneity of the sedimentation boundary observed in the velocity experiments.

Upon addition of Ca^{2+} or Mg^{2+}, the sedimentation coefficient assumes values of 2.85 and 3.16, respectively — more typical of globular proteins in the 25–30 kDa range. Accordingly, the Ca^{2+}-bound and Mg^{2+}-bound forms of CPV3 display apparent molecular weights of 26,700 and 28,400, respectively, in sedimentation equilibrium studies. Least-squares analysis of the equilibrium data suggests that addition of either metal ion changes the association from a predominantly monomer–dimer equilibrium to an exclusively monomer–trimer equilibrium.

For example, addition of Ca^{2+} increases the overall equilibrium constant for trimerization by nearly an order of magnitude, to 5.7×10^7 M^{-2}, while reducing β_2 to essentially zero. Using these values for the association constants, the calculated monomer, dimer, and trimer concentrations are 61, 0, and 39 μM, respectively, at a total protein concentration of 100 μM.

The larger sedimentation coefficient and apparent average molecular weight observed for Mg^{2+}-bound CPV3 imply that the association reaction is even more strongly favored in Mg^{2+}. As in the presence of Ca^{2+}, least-squares analysis of the sedimentation equilibrium data indicates that $\beta_2 = 0$. However, the optimal value for β_3 increases to 1.2×10^8 M^{-2}. Thus, at the point in the sedimentation cell where the total CPV3 concentration is 100 μM, the calculated monomer and trimer concentrations are 51 μM and 49 μM, and the dimer concentration is once again insignificant.

The implication that CPV3 forms a noncovalent trimeric species in the presence of Ca^{2+} or Mg^{2+} is relevant to the covalent oligomerization process described previously [18]. Upon exposure to air, in the absence of thiol-protecting reagents, Ca^{2+}-bound CPV3 forms disulfide-linked dimers over the course of many hours. Since C72 should be solvent-accessible in the Ca^{2+}-bound form of the protein, by analogy with S72 in oncomodulin [27,28], this result is consistent with expectation. However, substantial amounts of a trimeric form are also observed. In fact, when ferricyanide is employed as the oxidant, the trimeric form is the predominant species ([18]; Fig. 2B). The formation of covalent trimers requires participation of C18 in the covalent crosslinking process as well. Facile disulfide bond formation involving the largely inaccessible C18 thiol was puzzling, since the probability of a productive encounter between C72 and C18 through simple diffusion is expected to be extremely small.

However, the existence of a stable noncovalent trimeric complex in the presence of Ca^{2+} would greatly facilitate this reaction, provided that the noncovalent association brings C72 and C18 from neighboring subunits into sufficient proximity. Presumably, the trimeric species is more apparent when ferricyanide is employed as the oxidant because disulfide-bond formation is much more rapid under these conditions, resulting in an increased probability of forming both of the requisite covalent crosslinks before one of the subunits dissociates. Since the oxygen-mediated reaction is much slower, there is a greater probability of subunit dissociation occurring before both crosslinks have been formed.

Whereas the time course for covalent oligomerization is many hours, the self-association described herein is manifested

immediately during sedimentation velocity analysis. Moreover, whereas the covalent complexation is restricted to the Ca^{2+}-bound form of CPV3, noncovalent association is promoted by both Ca^{2+} and Mg^{2+}. These two observations strongly suggest that the sedimentation experiments are not simply detecting the covalent association reported earlier.

The X-ray structure determined for the highly homologous parvalbumin, oncomodulin, may be relevant to the CPV3 association problem [27,28]. In 10 mM Ca^{2+}, oncomodulin crystallizes in trimeric clusters, with three molecules liganded to an intermolecular Ca^{2+} ion. Whether Ca^{2+} serves to crosslink the subunits of the CPV3 trimer is presently unknown. However, the fact that the anomalous heat effects observed in titration calorimetry are complete with the addition of two equivalents of Ca^{2+} (H. Zhao and M.T. Henzl, unpublished observations) would suggest that this is not the case.

A highly speculative structure for the trimeric CPV3 complex is presented in Fig. 4. This model was derived manually, subject to the constraint that C18 and C72 from adjacent monomers be sufficiently close to permit disulfide bond formation. The view displayed in Fig. 4 was chosen to emphasize the symmetry of the complex. In (A), the cystine linkages have been retained and are shown in gray for emphasis. The same view is presented in (B) minus the disulfides, with the A helices and Ca^{2+}-binding loops colored gray to provide points of reference. Whether this structure has any basis in reality remains to be established. Efforts to crystallize CPV3 are currently underway. It is worth emphasizing that there must be a perceptible conformational difference between the trimeric complex formed in the presence of Ca^{2+} and the one formed in the presence of Mg^{2+}, since only the former appears capable of undergoing facile covalent oligomerization.

We have recently examined the intrathymic distribution of CPV3 in the chicken by confocal fluorescence microscopy, employing a fluorochrome-tagged monoclonal antibody to the protein (R.C. Hapak and M.T. Henzl, unpublished observations). Interestingly, a subset of the cortical thymocyte population exhibits peripheral staining, a finding consistent with the existence of cell-surface receptors for CPV3. Thus, the observed self-association of the protein could be physiologically significant, if the putative CPV3 receptors were specific for a trimeric form of the protein. Alternatively, the tendency to associate could facilitate receptor aggregation and receptor-mediated endocytosis subsequent to ligand–receptor engagement. The extracellular levels of Ca^{2+} and Mg^{2+} are both sufficient to favor CPV3 trimer formation.

Acknowledgments: The authors wish to thank Prof. William Morgan, Division of Biochemistry and Molecular Biology, University of Missouri at Kansas City, for the use of his Beckman XL-A analytical ultracentrifuge. This work was supported by NSF Award DCB92-96171 (to M.T.H.).

References

[1] Wnuk, W., Cox, J.A. and Stein, E.A. (1982) Calcium Cell Funct. 2, 243–278.
[2] Gerday, C. (1988) in Calcium and Calcium-Binding Proteins. Molecular and Functinoal Aspects (Gerday, Ch., Gilles, R. and Bolis, L. eds.) pp 23–39, Springer-Verlag, Berlin.
[3] Heizmann, C.W. (1984) Experentia 40, 910–921.
[4] MacManus, J.P. (1979) Cancer Res. 39, 3000–3005.
[5] MacManus, J.P. and Whitfield, J.F. (1983) Calcium Cell Funct. 4, 411–440.
[6] Blum, J.K. and Berchtold, M.W. (1994) J. Cell. Phys. 160, 455–462.
[7] Barger, B.O., Pace, J.L., Inman, F.P. and Ragland, W.L. (1977) Fed. Proc. 36, A1237.
[8] Pace, J.L., Barger, B.O., Dawe, D.L. and Ragland, W.L. (1978) Eur. J. Immunol. 8, 671–678.
[9] Murthy, K.K. and Ragland, W.L. (1984) in Chemical Regulation of Immunity in Veterinary Medicine, pp. 481–491, Alan R. Liss, New York.
[10] Murthy, K.K., Beach, F.G. and Ragland, W.L. (1984) in: Thymic Hormones and Lymphokines (Goldstein, A.L. ed.) pp. 375–382.
[11] Hall, C.A., Beach, G.G. and Ragland, W.L. (1991) Hybridoma 10, 575–582.
[12] Kiraly, E. and Celio, M.R. (1993) Anat. Embryol. 88, 339–344.
[13] Henzl, M.T., Serda, R.E. and Boschi, J.M. (1991) Biochem. Biophys. Res. Commun. 177, 881–887.
[14] Haiech, J., Derancourt, J., Pechere, J.-F. and Demaille, J.G. (1979) Biochemistry 18, 2752–2758.
[15] Moeschler, H.J., Schaer, J.-J. and Cox, J.A. (1980) Eur. J. Biochem. 111, 73–78.
[16] Serda, R.E. and Henzl, M.T. (1991) J. Biol. Chem. 266, 7291–7199.
[17] Hapak, R.C., Zhao, H., Boschi, J.M. and Henzl, M.T. (1994) J. Biol. Chem. 269, 5288–5296.
[18] Hapak, R.C., Zhao, H. and Henzl, M.T. (1994) FEBS Lett. 349, 295–300.
[19] Haner, M., Henzl, M.T., Raissouni, B. and Birnbaum, E.R. (1984) Anal. Biochem. 138, 229–234.
[20] Palmisano, W.A., Treviño, C.L. and Henzl, M.T. (1990) J. Biol. Chem. 265, 14450–14456.
[21] Ellman, G.L. (1959) Arch. Biochem. Biophys. 82, 70–77.
[22] Lewis, M.S. and Youle, R.J. (1986) J. Biol. Chem. 261, 11571–11577.
[23] Cantor, C.R. and Schimmel, P.R. (1980) Biophysical Chemistry, part II, Freeman and Co., San Francisco, pp. 591–641.
[24] Squire, P.G. and Himmel, M.E. (1979) Arch. Biochem. Biophys. 196, 165–177.
[25] Padilla, A., Cavé, A. and Parello, J. (1988) J. Mol. Biol. 204, 995–1017.
[26] Henzl, M.T., Likos, J.J. and Hutton, W.C. (1995) Protein Sci. 4 (suppl. 2), 477-M.
[27] Ahmed, F.R., Przybylska, M., Rose, D.R., Birnbaum, G.I., Pippy, M.E. and MacManus, J.P. (1990) J. Mol. Biol. 216, 127–140.
[28] Ahmed, F.R., Rose, D.R., Evans, S.V., Pippy, M.E. and To, R. (1993) J. Mol. Biol. 230, 1216–1224.